Supporting Information

Sanchez et al. 10.1073/pnas.1121081109

Materials and Methods

Morris Water Maze. The maze consisted of a pool (122-cm diameter) filled with water (21 ± 1 °C) made opaque with nontoxic white tempera paint powder. The pool was located in a room surrounded by distinct extramaze cues. Before hidden-platform training, mice were given two pretraining trials in which they had to swim in a rectangular channel (15 cm × 122 cm) and mount a platform hidden 1.5 cm below the surface in the middle of the channel. Mice that did not mount the platform were guided to it gently and were allowed to sit on it for 10 s before being removed by the experimenter. The maximum time allowed per trial in this task was 90 s. The day after pretraining, mice were trained in the circular water maze. For hidden-platform training, the platform (14 × 14 cm) was submerged 1.5 cm below the surface. The platform location remained the same throughout hidden-platform training, but the drop location varied semirandomly among trials. Mice received two training sessions with a 3-h intersession interval for 5 d consecutively. Each session consisted of two trials with a 30-min intertrial interval. The maximum time allowed per trial in this task was 60 s. If a mouse did not find the platform, it was guided to it and allowed to sit on it for 10 s. For the probe trial, the platform was removed, and mice were allowed to swim for 60 s before they were removed. The drop location for probe trials was 180° from the platform location during hidden-platform training. After the probe trial, mice were allowed to rest for 1 d before visible-platform training was performed. In the visible-platform task, the platform location was marked with a visible cue (a black-and-white striped pole 15 cm tall) placed on top of the platform. Mice received two training sessions/d with a 3- to 4-h intersession interval. Each session consisted of two training trials with a 30-min intertrial interval. The maximum time allowed per trial in this task was 60 s. For each session, the platform was moved to a new location, and the drop location varied semirandomly among trials.

Immunohistochemistry. Mice were anesthetized with Avertin (tribromoethanol, 250 mg/kg) and transcardially perfused with 0.9% saline. Immunohistochemistry was performed on floating 30-μm-thick microtome sections. Primary antibodies were rabbit anti-calbindin (1:20,000; Swant), rabbit anti-Fos (1:4,000; Ab-5; Calbiochem), rabbit anti-neuropeptide Y (NPY) (1:8,000; Immunostar), and mouse biotinylated anti-3D6 (1:1,000; Elan Pharmaceuticals). Binding of the nonbiotinylated primary antibodies was detected with biotinylated donkey anti-rabbit (1:1,000; Jackson ImmunoResearch) followed by incubation with avidin-biotin complex (Vector Laboratories). For all immunostaining, diaminobenzidine was used as the chromagen. Images were acquired with a digital microscope (Axiocam; Carl Zeiss). Fos, calbindin, and NPY immunoreactivities were quantified as described (1). The number of amyloid-β (Aβ) deposits in the hippocampus and cortex was counted in three 3D6-immunostained coronal brain sections per mouse.

Immunoblotting. For Western blot analysis of calbindin and α-tubulin, 20 μg of protein was loaded into each well of a 4–12% gradient SDS/PAGE gel. After electrophoresis, gels were transferred to nitrocellulose membranes that were immunoblotted with rabbit anti-calbindin (1:30,000; Swant) or mouse anti–α-tubulin (1:1,000,000; Sigma). Goat anti-rabbit or anti-mouse antibodies (1:5,000; Calbiochem; room temperature, 1 h) were used as secondary antibodies. For Western blot analysis of full-length human amyloid precursor protein (hAPP) and hAPP C-terminal fragments, 50 μg of protein from parietal cortex lysates was loaded into each well of a 10–20% Tris-tricine gel (Bio-Rad). After electrophoresis, gels were transferred to nitrocellulose membranes that were immunoblotted with mouse anti-8E5 to detect full-length hAPP (1:10,000; Elan Pharmaceuticals), rabbit CT15 to detect C-terminal fragments (1:5,000; kindly provided by Edward Koo, University of California at San Diego, La Jolla, CA), or mouse α-tubulin (1:1,000,000; Sigma). Goat anti-rabbit or anti-mouse antibodies (1:5,000, Chemicon) (room temperature, 2 h) were used as secondary antibodies. Protein bands were visualized with an ECL system (Pierce), and their intensity was quantified by densitometry.

Acute Brain Slices. Mice were decapitated, and brains were removed quickly and immersed in ice-cold cutting solution containing (in mM) 234 sucrose, 2.5 KCl, 1.25 NaH_2PO_4, 10 $MgSO_4$, 26 $NaCO_3$, 11 glucose, and 1.3 ascorbic acid, and oxygenated with 95% O_2/5% CO_2. Transverse 400-μm slices were cut on a Vibratome 3000 slicer (Leica) and were incubated at 32 °C for 30 min in an interface incubation chamber (Automated Scientific). The incubation continued at room temperature for another hour before each slice was transferred to a submerged recording chamber and perfused continuously with oxygenated artificial cerebrospinal fluid (aCSF) containing (in mM) 126 NaCl, 2.5 KCl, 1.25 NaH_2PO_4, 1 $MgSO_4$, 26 $NaHCO_3$, 10 glucose, and 2 CaCl2 at 3 mL/min (31–32 °C). Slices were allowed to equilibrate for 10–20 min in the recording chamber before the recording began.

Electrophysiology. For field potential recordings, a bipolar stimulating electrode made of platinum-iridium (FHC Inc.) was placed halfway between the end of the granule cell layer and the vertex of the two blades of the dentate gyrus, ~30 μm from the granule cell layer of the dorsal blade, to stimulate the medial perforant pathway. Field excitatory postsynaptic potentials (fEPSPs) were recorded with glass electrodes (2–3 MΩ) filled with aCSF and placed at the same distance from the granule cell layer but 350–400 μm closer to CA3. Both electrodes were advanced into the slice in 10-μm steps until a maximal response was recorded. Test stimuli of 100-μs duration and varying intensity (40–200 μA) were delivered from a Master 8 stimulator (A.M.P.I.). Stimulus was delivered at 0.033 Hz. Stimulation of the medial perforant path was confirmed by paired-pulse depression at the beginning of each experiment. A 15-min stable baseline of fEPSP was established at an intensity that evoked ~40% of the maximal response before induction of long-term potentiation (LTP). The means of every three fEPSPs were used for final analysis and plotting. LTP was induced by theta-burst protocol (four trains delivered every 20 s, each train containing 10 bursts at 5 Hz, and each burst containing four pulses at 200 Hz). Bicuculline (2.5 μM; Tocris) was included in the aCSF to facilitate induction of LTP. Recording electrodes were pulled from borosilicate glass capillaries (WPI Inc.) on a horizontal microelectrode puller (P-97; Sutter Instruments). fEPSP recordings were filtered at 2 KHz, digitized at 20 kHz by a Multiclamp 700A amplifier (Axon Instruments), and acquired with a Digidata-1322A digitizer and pClamp 9.2 software (Axon). Offline analysis was done with Pclamp 9.2, WinLTP program (University of Bristol) and Original pro 8.0 (Origin Labs).

In Vivo Aβ Microdialysis. In vivo Aβ microdialysis samples soluble molecules within the extracellular fluid that are smaller than 30 kD,

the molecular-weight cutoff (MWCO) of the probe membrane. Aβ capable of entering the probe has been dubbed "exchangeable Aβ" or "eAβ" (2). Under isoflurane volatile anesthetic, a guide cannula (BR style; Bioanalytical Systems) was cemented into the left hippocampus (stereotaxic coordinates: 3.1 mm behind bregma, 2.5 mm lateral to midline, and 1.2 mm below dura at a 12° angle). Two-millimeter microdialysis probes were inserted through the guides so that the BR-2, 30-kD MWCO membrane (Bioanalytical Systems) was contained entirely within the hippocampus. Microdialysis perfusion buffer was aCSF (in mM: 1.3 $CaCl_2$, 1.2 $MgSO_4$, 3 KCl, 0.4 KH_2PO_4, 25 $NaHCO_3$, and 122 NaCl, pH 7.35) containing 4% BSA (by weight; Sigma) that was filtered through a 0.1-μM membrane. Mice recovered for 6–8 h after probe insertion followed by an interpolated zero-flow protocol (3) to determine the absolute concentrations of interstitial fluid Aβ in each mouse essentially as described (2). Flow rate was varied from 0.1 μL/min to 2.0 μL/min in each mouse. Samples were collected with a refrigerated fraction collector into polypropylene tubes every 45–360 min (collection time was inversely related to flow rate). The concentration of Aβx-40 and Aβx-42 in each microdialysis sample was measured by sandwich ELISA as described (4). An exponential trend line was fitted based on the concentration of Aβ in each sample versus flow rate with the line projected back to a theoretical zero flow rate. The Aβ concentration at the zero flow rate should represent the concentration at which Aβ inside and outside the probe are in equilibrium and thus should be equal to the in vivo concentration of Aβ within the brain's interstitial fluid (3).

1. Palop JJ, Mucke L, Roberson ED (2011) Quantifying biomarkers of cognitive dysfunction and neuronal network hyperexcitability in mouse models of Alzheimer's disease: Depletion of calcium-dependent proteins and inhibitory hippocampal remodeling. *Methods Mol Biol* 670:245–262.
2. Cirrito JR, et al. (2003) In vivo assessment of brain interstitial fluid with microdialysis reveals plaque-associated changes in amyloid-beta metabolism and half-life. *J Neurosci* 23:8844–8853.
3. Menacherry S, et al. (1992) In vivo calibration of microdialysis probes for exogenous compounds. *Anal Chem* 64:577–583.
4. Verges DK, Restivo JL, Goebel WD, Holtzman DM, Cirrito JR (2011) Opposing synaptic regulation of amyloid-β metabolism by NMDA receptors in vivo. *J Neurosci* 31:11328–11337.

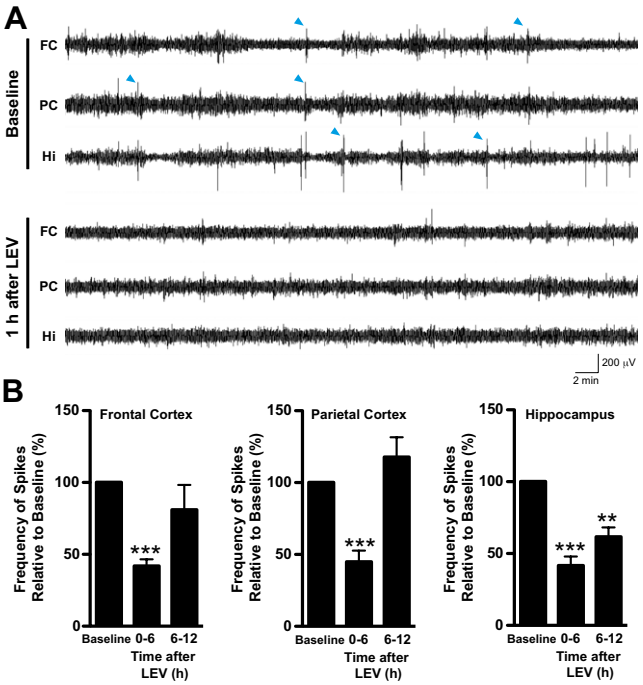

Fig. S1. Levetiracetam (LEV) decreases abnormal spike activity in several brain regions of hAPP mice. To record EEG at multiple sites, subdural electrodes were placed bilaterally over the parietal and frontal cortices and implanted within the hippocampus (stereotaxic coordinates: mediolateral, ± 1.66 mm and anteroposterior, ± 2.46 mm from bregma; dorsoventral, −1.87 mm from the skull surface). EEGs were recorded in hAPPJ20 mice before and after acute injection of LEV (200 mg/kg, i.p.; $n = 3$ mice). The number of spikes per hour was quantified as described in Fig. 1. (*A*) Representative recordings showing abnormal spike activity in different brain regions of an untreated hAPP mouse. LEV injection transiently suppressed spike activity as illustrated by the marked suppression of spikes in an hAPP mouse 1 h after LEV injection. FC, frontal cortex; PC, parietal cortex; Hi, hippocampus. (*B*) During the first 6 h after the injection, LEV reduced the number of spikes in hAPP mice in all brain regions to a similar extent (by ∼60% on average). Subsequently, the frequency of spikes increased, returning to baseline levels by 6–12 h after the injection in the frontal and parietal cortices. In the hippocampus, the spike frequency was still significantly reduced 6–12 h after the injection. Baseline EEGs were recorded for 24 h. $^{**}P < 0.005$, $^{***}P < 0.0005$ vs. baseline (repeated-measures one-way ANOVA and Bonferroni test). Values in *B* are means ± SEM.

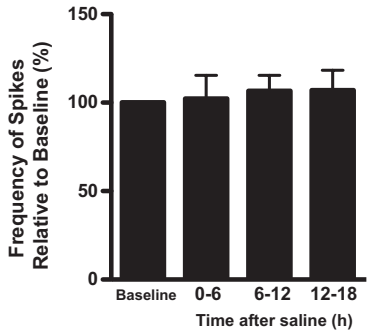

Fig. S2. Saline injection has no effect on abnormal spike activity in hAPP mice. Subdural EEG was recorded from the parietal cortex in hAPPJ20 mice (n = 5) before and after acute i.p. injection of saline. Saline injection had no effect on the frequency of spikes (one-way ANOVA). Values are means ± SEM.

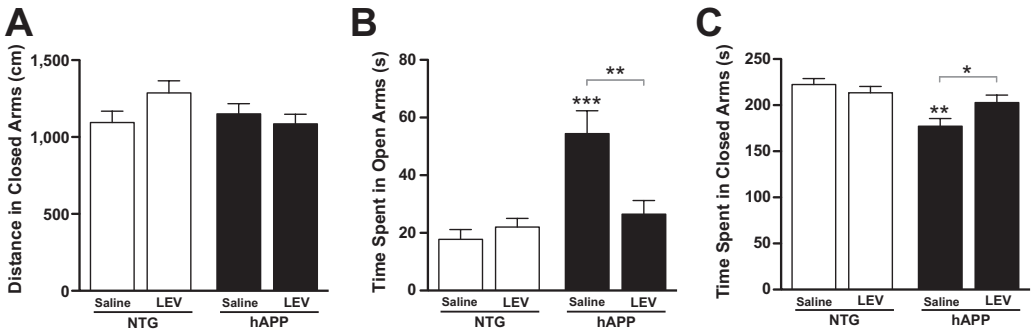

Fig. S3. LEV treatment reverses behavioral abnormalities of hAPPJ20 mice in the elevated plus maze. Behavioral testing was performed in two independent cohorts of 4- to 6-mo-old mice. Because results were similar in both cohorts, the data were pooled. hAPP mice and nontransgenic (NTG) controls were chronically treated s.c. with saline or LEV (75 mg·kg^{-1}·d^{-1}, n = 21–30 mice per genotype and treatment). Mice were tested in the elevated plus maze 19 d (cohort 1) or 5 d (cohort 2) after the start of treatment. (*A*–*C*) Distance traveled in closed arms (*A*) and time spent in open (*B*) and closed (*C*) arms. Two-way ANOVA revealed a significant interaction between genotype and treatment (*B*, P = 0.008; *C*, P = 0.04). *P < 0.05, **P < 0.005, ***P < 0.0005 vs. saline-treated NTG or as indicated by bracket (Bonferroni test). No significant differences were detected between groups in the distance they moved in the closed arms (two-way ANOVA). Values are means ± SEM.

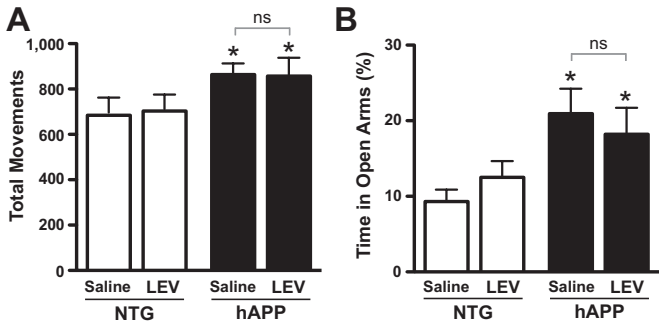

Fig. S4. A single injection of LEV does not reverse behavioral abnormalities in hAPP mice. (*A*) NTG and hAPPJ20 mice (n = 12–17 mice per group for each test) received a single i.p. injection of saline or LEV (200 mg/kg) and were tested 2 h later in the open field. (*B*) Three days later, the same groups of mice were injected again i.p. with saline or LEV (200 mg/kg) and were tested 2 h later in the elevated plus maze. Two-way ANOVA revealed a significant effect of genotype (*A*, P = 0.009; *B*, P = 0.0046) but not of treatment (*A*, P = 0.17; *B*, P = 0.43) and no interaction between genotype and treatment (*A*, P = 0.15; *B*, P = 0.17). *P < 0.05 vs. saline-treated NTG (Bonferroni test). Values are means ± SEM. ns, not significant.

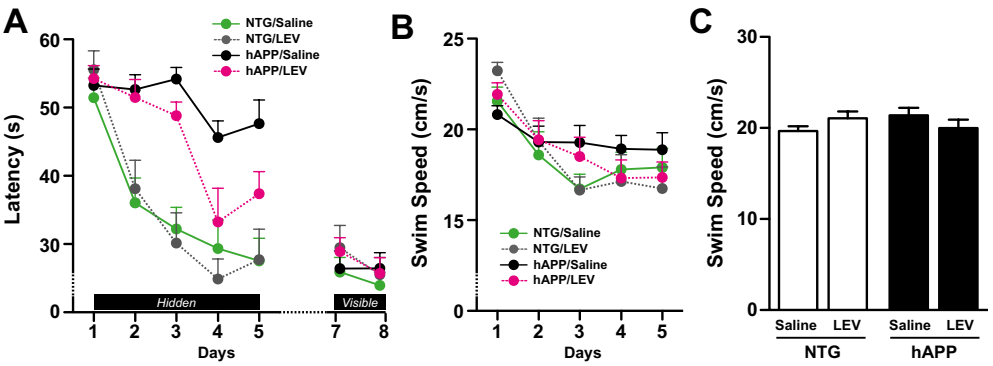

Fig. S5. LEV treatment ameliorates spatial learning deficits in hAPP mice. hAPPJ20 mice and NTG controls were chronically treated with saline or LEV (75 mg·kg^{-1}·d^{-1}, s.c., for 20 d). (*A*) Learning curves during training in the Morris water maze (n = 10–15 mice per genotype and treatment). The latency for each mouse to reach the hidden or cued platform was recorded. Data points represent the average performance of mice during four training trials/d. For the hidden-platform component, repeated-measures ANCOVA revealed a significant interaction between genotype and day in saline-treated NTG and hAPP mice (P = 0.0086) and a significant interaction between LEV treatment and day in hAPP mice (P = 0.043) but not in NTG controls. (*B* and *C*) Swim speed was recorded during the hidden-platform training (*B*) and the probe trial (*C*). No differences in swim speed were detected among groups by two-way ANOVA. Values are means ± SEM.

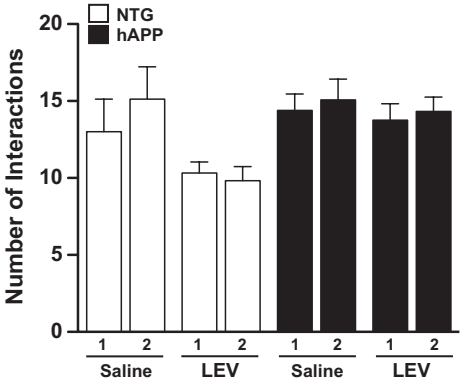

Fig. S6. Mice showed no object preference during the training session of the novel object paradigm. hAPPJ20 mice and NTG controls were chronically treated with saline or LEV (75 mg·kg^{-1}·d^{-1}, s.c., for 22 d) and were then tested in a novel object recognition paradigm (n = 9–13 mice per genotype and treatment). The number of times mice interacted with the two objects (1 and 2) was recorded for 10 min. In the training session, none of the groups preferred one object over the other (unpaired t test). Values are means ± SEM.

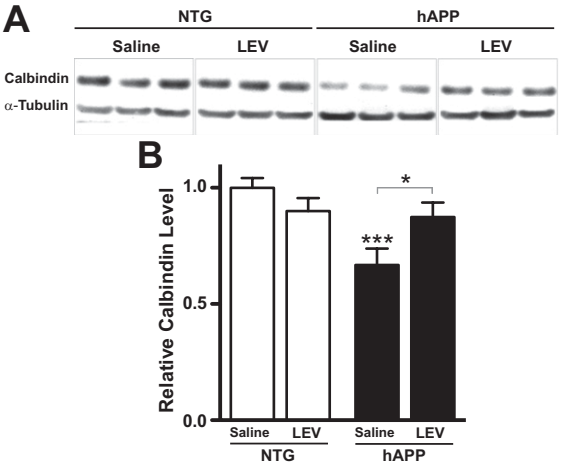

Fig. S7. LEV treatment improves calbindin levels in the dentate gyrus of hAPP mice. Dentate gyri from NTG and hAPPJ20 mice treated s.c. with saline or LEV (75 mg·kg^{-1}·d^{-1}) for 28 d (n = 10–15 mice per group) were dissected, and calbindin levels were determined by Western blot analysis; α-tubulin served as a loading control. (*A*) Representative Western blots of dentate gyrus lysates illustrating levels of calbindin and α-tubulin. (*B*) Relative calbindin levels normalized to α-tubulin. Two-way ANOVA revealed a significant interaction between genotype and treatment (P = 0.037). *P < 0.05, ***P < 0.0005 vs. saline-treated NTG or as indicated by bracket (Bonferroni test). Values are mean ± SEM.

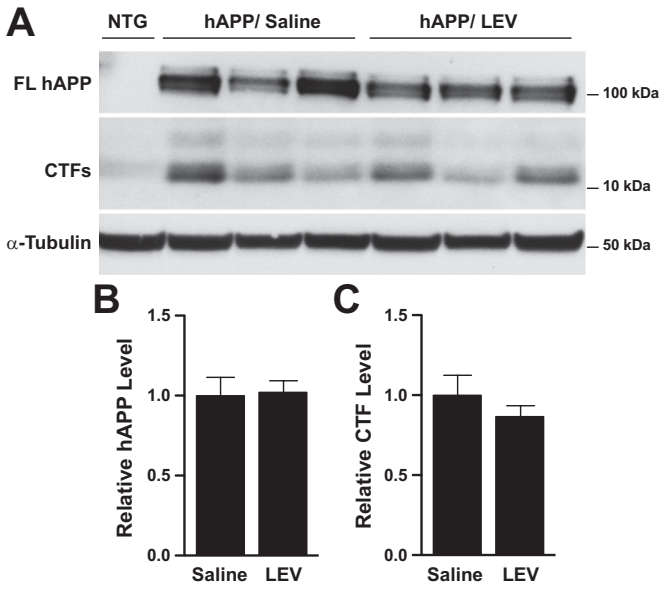

Fig. S8. Chronic LEV treatment does not alter levels of full-length hAPP or hAPP C-terminal fragments in hAPP mice. Parietal cortices from NTG and hAPPJ20 mice treated s.c. with saline or LEV (75 mg·kg^{-1}·d^{-1}) for 28 d (n = 10–15 mice per group) were dissected, and levels of full-length (FL) hAPP and hAPP C-terminal fragments (CTFs) were determined by Western blot analysis. α-Tubulin served as a loading control. (*A*) Representative Western blots of cortical lysates illustrating levels of full-length hAPP, C-terminal fragments, and α-tubulin. (*B* and *C*) Quantitation of relative levels of full-length hAPP (*B*) and C-terminal fragments (*C*), which were unchanged by LEV treatment (unpaired t test). Values are means ± SEM.

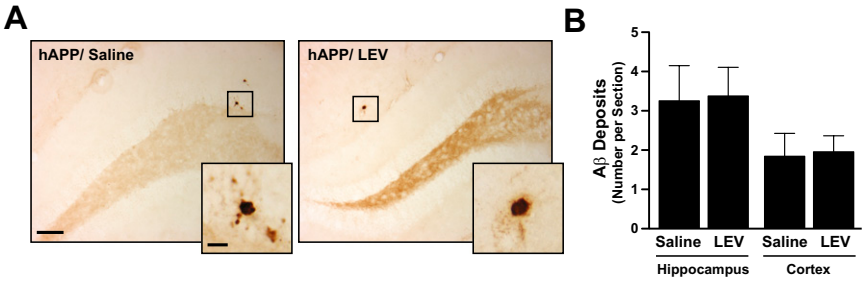

Fig. S9. Chronic LEV treatment does not alter early Aβ deposition in hAPP mice. Coronal brain sections from 5- to 6-mo-old hAPPJ20 mice treated s.c. with saline or LEV (75 mg·kg^{-1}·d^{-1}) for 28 d (n = 10–15 mice per group) were immunostained with the anti-Aβ antibody 3D6. (*A*) Representative photomicrographs of hippocampus showing small Aβ deposits at low and high magnification. (Scale bars: 100 μm, low magnification; 20 μm, high magnification.) (*B*) Number of Aβ deposits (average from three sections per mouse) in the hippocampus and cortex. Values are means ± SEM.